



HAL
open science

Pt/carbon xerogel catalysts for PEM fuel cells

Nathalie Job, Frédéric Maillard, Jean-Paul Pirard, Sandrine Berthon-Fabry,
Marian Chatenet

► **To cite this version:**

Nathalie Job, Frédéric Maillard, Jean-Paul Pirard, Sandrine Berthon-Fabry, Marian Chatenet. Pt/carbon xerogel catalysts for PEM fuel cells. *Fundamentals & Developments of Fuel Cells (FDFC) 2011 Conference*, Jan 2011, Grenoble, France. 8 p. - ISBN 978-2-7466-2972-7. hal-00800928

HAL Id: hal-00800928

<https://minesparis-psl.hal.science/hal-00800928>

Submitted on 14 Mar 2013

HAL is a multi-disciplinary open access archive for the deposit and dissemination of scientific research documents, whether they are published or not. The documents may come from teaching and research institutions in France or abroad, or from public or private research centers.

L'archive ouverte pluridisciplinaire **HAL**, est destinée au dépôt et à la diffusion de documents scientifiques de niveau recherche, publiés ou non, émanant des établissements d'enseignement et de recherche français ou étrangers, des laboratoires publics ou privés.

Pt/CARBON XEROGEL CATALYSTS FOR PEM FUEL CELLS

Nathalie JOB^a, Frédéric MAILLARD^b, Jean-Paul PIRARD^a,
Sandrine BERTHON-FABRY^c, Marian CHATENET^b

^aLaboratoire de Génie Chimique, Université de Liège, B6a, B-4000 Liège, Belgium

^bLEPMI, UMR 5631 CNRS/Université de Grenoble, BP75, F-38402 St Martin d'Hères Cedex, France

^cMines ParisTech, Centre Énergétique et Procédés, BP 207, F-06904 Sophia-Antipolis Cedex, France

ABSTRACT

Carbon xerogels have been used to replace carbon black as catalyst support at the cathode of proton exchange membrane (PEM) fuel cells in order to decrease the mass transport limitations in this electrode. Carbon xerogels are very clean nanostructured carbons with well-defined pore texture, which allows for better reactant/product diffusion. Pt/carbon xerogel catalysts with high metal dispersion (nanoparticles *ca.* 2 nm in size) and high metal content (~ 25 wt.%) can be engineered *via* rational synthesis methods such as the 'Strong Electrostatic Adsorption' technique. The results show that choosing correctly the average pore texture of the carbon xerogel allows for minimizing the diffusion overpotential of the H₂/air cell. However, the catalyst characterization indicates that the presence of chlorine, coming from H₂PtCl₆, induces a dramatic decrease of the Pt utilization ratio in the final PEMFC catalytic layer. To remove chlorine, a reduction of the catalyst at 450°C, at least, is necessary.

1. INTRODUCTION

The catalytic layer configuration is a key-element in the design of PEM fuel cells [1]. Indeed, besides the characteristics of the chosen catalyst (composition, crystallographic structure, dispersion, connectivity with the membrane, etc.), the structure of the catalytic layer itself affects the mass transfer phenomena in the electrodes as well as their intrinsic reactivity [2]. To reach high performance, reactants and products should be able to circulate easily through the catalytic layers: (i) the catalyst must be accessible to the gas reactant, through the percolating porous structure of the catalytic layer; (ii) protons and electrons need to be collected by the ionomer and the catalyst support, respectively, and driven to the membrane (protons) and the current collector (electrons) [2]. Thus, the optimisation of mass transfer inside the electrodes is one of the foreseen ways to increase fuel cell performances [1].

Carbon blacks, commonly used for the preparation of the catalysts, are formed of primary carbon particles (~50 nm) assembled together as agglomerates (1 – 100 µm) [3]. The pore structure of the catalytic layers strongly depends on the packing of these agglomerates; as a consequence, the choice of the carbon black used as well as the electrode processing influence the mass transport phenomena. Typically, at the air-fed cathode, where the transport of oxygen, protons and water are involved in the oxygen reduction reaction (ORR), high potential losses due to diffusion limitations offset the cell performance. To cope with this problem, PEM fuel cell designers generally use catalysts with very high platinum loadings (50 wt.% and more), which enables one to prepare thin catalytic layers with acceptable diffusion-induced potential losses. However, reducing the Pt loading of PEMFC electrodes is one of the requirements to reach commercially viable PEMFCs.

This major drawback calls for the development of new carbon materials with controllable and tunable pore texture. In addition, and especially for electrochemical applications, high purity of the carbon supports is also essential [4]. The goal of the present work is to design new Pt/C catalysts using a support with adapted pore structure. Recently, it was envisaged to replace carbon blacks by carbon gels, *i.e.* synthetic porous carbons. In particular, carbon xerogels prepared by evaporative drying and pyrolysis of resorcinol-formaldehyde aqueous gels [5, 6] proved to be efficient as catalyst and electrocatalyst supports [7-9]: these materials are very clean nanostructured carbons with well defined pore size, which is easily tunable between a few nm and a few µm. This pore texture allows for better fluid diffusion in catalyzed processes [7]. The present paper aims at showing the advantages of carbon gels as electrocatalyst supports for PEM fuel cell electrodes.

2. EXPERIMENTAL

2.1. Catalyst preparation

Carbon supports were synthesized by the drying and pyrolysis of resorcinol-formaldehyde aqueous gels, following a procedure developed in a previous study [6]. The procedure consists of the polycondensation of resorcinol (R) with formaldehyde (F) in a solvent (water), followed by evaporative drying and pyrolysis. Globally, the pore texture of the final carbon is fixed by the pH of the solution, which is adjusted by adding a basification agent, usually sodium carbonate (C). In most works dealing with RF carbon gels, the pH adjustment is reported through the resorcinol/sodium carbonate molar ratio, R/C . In the present work, R/C was chosen equal to 750, 1000 and 2000 while all other synthesis variables (from gel preparation to pyrolysis conditions) were kept identical as in the above-mentioned study. In brief, resorcinol and sodium carbonate were solubilized in water, prior to formaldehyde addition. Gelation and ageing were performed at 85°C (72 h), followed by evaporative drying (60-150°C, 1 day) and pyrolysis (800°C, 2 h) under nitrogen flow.

Fig. 1 shows the evolution of the pore texture of carbon xerogels with R/C . Scanning electron microscopy (SEM) micrographs of carbon xerogels presenting extreme morphologies are shown on Fig. 1a and 1b. Carbon xerogels are materials composed of interconnected spherical-like microporous nodules. So, they classically display a bimodal pore size distribution: micropores inside the carbon nodules, and larger pores identified as the voids located between the nodules [5, 6]. The size of the nodules and that of the voids in-between is controlled by the synthesis conditions of the pristine gel, and particularly by the pH of the precursors' solution [5, 6]. Fig. 1c reports the mesopore size distribution of three carbon xerogels prepared and tested in this study: the average meso/macropore size is of *ca.* 30 nm ($R/C = 750$), 60 nm ($R/C = 1000$) and 200 nm ($R/C = 1000$). The meso/macropore volume increases with R/C (1.3, 2.1 and 2.2 $\text{cm}^3 \text{g}^{-1}$, respectively), while the volume of micropores remains nearly constant ($\sim 0.26 \text{ cm}^3 \text{g}^{-1}$). This micropore volume corresponds to a specific surface area of about 650 $\text{m}^2 \text{g}^{-1}$.

Pt/carbon xerogel catalysts were obtained *via* the ‘Strong Electrostatic adsorption’ (SEA) method [10]. This method consists of maximizing the electrostatic interactions between the metal precursor and the support by adjusting the pH of the slurry to the adequate value, the latter depending on the surface chemistry of the carbon and on the precursor chosen. Indeed, interaction between the support and the metal precursor depends on both the precursor nature (anion or cation, size, etc.) and on the carbon surface chemistry [10].

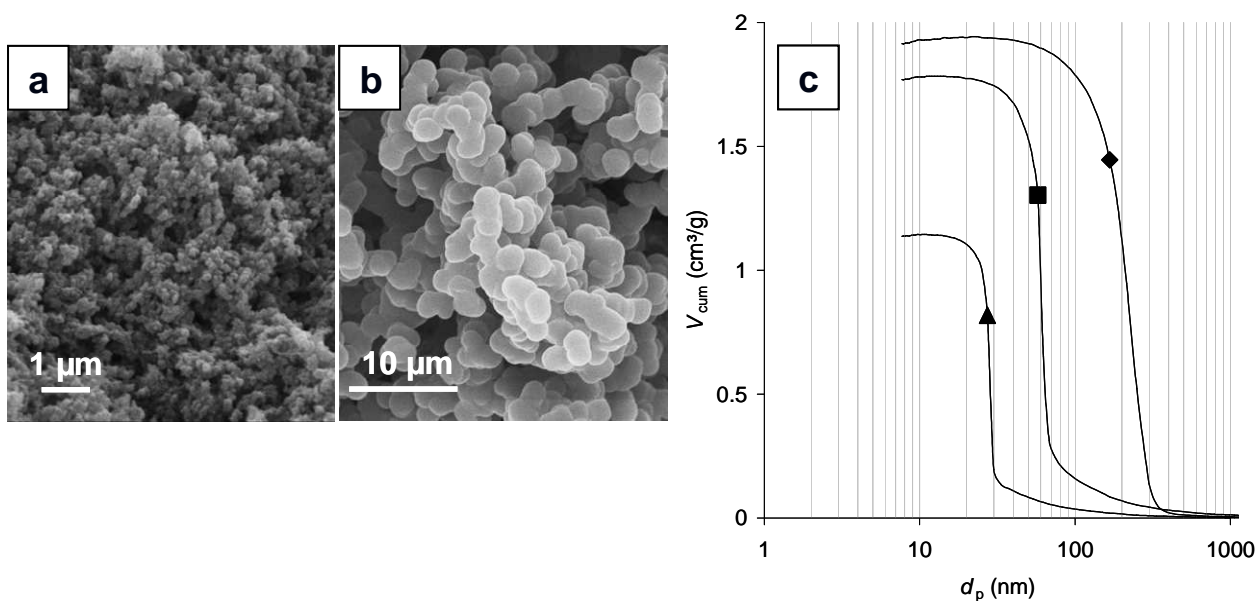


Figure 1. Morphology of carbon xerogels. SEM micrographs of carbon xerogels prepared at $R/C = 500$ (pH ~ 6.5) (a) and $R/C = \infty$ (pH ~ 4.0), *i.e.* without basification agent (b). Meso/macropore size distribution of carbon xerogels prepared at $R/C = 750$ (▲), 1000 (■) and 2000 (◆), determined by mercury porosimetry.

At pH values lower than the Point of Zero Charge (PZC), *i.e.* the pH at which the surface is neutral in terms of charge, the surface is positively charged, and the adsorption of anions is favoured. At pH higher than the PZC, the surface is negatively charged, and the adsorption of cations is enhanced. However, the metal uptake is limited by steric and repulsive effects [10]. As a consequence, depending on the support chemistry and metal precursor, one can define a pH window leading to a maximum uptake of metal. In a previous work [11], it was shown that the initial pH leading to the highest Pt uptake is equal to 2.5 (final pH at equilibrium \sim 3.0) for the impregnation of carbon xerogels with H_2PtCl_6 aqueous solutions (1000 ppm_{Pt}); the corresponding maximum weight percentage per impregnation step ranges from 8 to 10 wt.% [11]. In that frame, the Pt/carbon xerogels were elaborated *via* the SEA method, as fully described in reference [9]. Briefly, the carbon support was contacted with the impregnation solution (H_2PtCl_6 aqueous solution, 1000 ppm_{Pt}) at the optimal pH value of 2.5 until the equilibrium was reached. The impregnated catalyst was then filtered, dried and reduced under flowing hydrogen (200°C, 1 h). In order to increase the Pt weight percentage up to acceptable values for electrochemical applications, this impregnation-drying-reduction cycle was repeated up to three times using the same original catalyst batch. Note also that various final reduction temperatures (200, 350 and 450°C after the last impregnation cycle) were tested.

2.2. Catalyst characterization

2.2.1. Physico-chemical characterization

The pore texture of the carbon supports were characterized by classical methods, such as nitrogen adsorption-desorption and mercury porosimetry. These techniques give access to the specific surface area, the pore volume (micropores < 2 nm, mesopores between 2 and 50 nm and macropores > 50 nm) and pore size distribution. The methods for obtaining the pore texture characteristics of carbon xerogels are fully described elsewhere [5, 6].

The catalysts were characterized using several complementary techniques. The Pt content was evaluated by ICP-AES after elimination of the carbon and solubilisation of the metal [12]. The size of the metal particles was investigated by transmission electron microscopy (TEM), with a Jeol 2010 (200 kV) device (LaB₆ filament). The samples were crushed and dispersed in ethanol and subsequently deposited onto a copper grid bearing a lacey carbon membrane. Particle size distributions were obtained by image analyses performed on a set of at least 1000 particles, as described in [9]. The samples were analyzed by X-ray photoelectron spectroscopy (XPS), performed on an SSI-X-probe (SSX-100/206) spectrometer from Fisons [9].

2.2.2. Electrochemical characterization

All electrochemical measurements were carried out in sulphuric acid (1 M) at 25°C. The voltammetric experiments were performed using an Autolab-PGSTAT20 potentiostat with a three-electrode cell and a saturated calomel electrode (SCE) as a reference electrode (+0.245 V *vs.* normal hydrogen electrode, NHE). The catalyst sample was deposited on a rotating disk electrode (EDT 101, Tacussel), used as working electrode. All details, from sample preparation to experimental conditions, are extensively described in reference [9].

The electrochemically active Pt surface area of the catalysts, $S_{\text{Pt-Strip}}$, was determined by CO stripping, assuming that the electrooxidation of a CO_{ads} monolayer requires 420 μC per cm^2 of Pt. Since CO stripping is performed in aqueous electrolyte, it implies 100% utilization of the Pt surface atoms and is influenced neither by contact problems between the metal and the electrolyte nor by mass-transport limitations. In addition, the electrooxidation of a CO_{ads} monolayer is a structure-sensitive reaction and provides a wealth of information on the particle size distribution and the presence/absence of particle agglomeration [12, 13]. The CO stripping voltammograms were recorded at 0.02 V s^{-1} between +0.045 and +1.245 V *vs.* NHE, after saturation of the electrolyte by CO (6 min bubbling) and removal of the non-adsorbed CO from the cell by purging with Ar (39 min).

The electrocatalytic activity for the ORR of the elaborated Pt/C nanoparticles was measured in O_2 -saturated liquid electrolyte. The quasi-steady-state voltammograms were recorded at 10^{-3} V s^{-1} from +1.095 to +0.245

V vs. NHE. To account for the reactants diffusion-convection in the liquid layer, the experiment was repeated at four RDE rotation speeds (42, 94, 168 and 262 rad s⁻¹) [14]. The results are reported in terms of (i) Tafel slope, b , and (ii) specific activity at 0.90 V vs. NHE, SA_{90} . This potential corresponds to 0.34 V ORR overpotential in 1 M sulphuric acid, a value classically monitored in a PEMFC cathode at low current densities, *i.e.* under kinetic control.

2.2.3. Fuel cell test

The catalysts were tested as PEM fuel cell cathodic catalytic layers on a unit cell-test bench: 50 cm² Membrane-Electrode Assemblies (MEAs) were prepared by the decal method as described in reference [8]. The electrolyte was a Nafion[®] membrane, and the anode a commercial anode made from Pt-doped carbon black (40 wt.%, TKK) deposited by Paxitech onto a carbon felt (0.6 mg_{Pt} cm⁻² mixed with Nafion[®]). The thickness of the cathode was kept constant by keeping constant the carbon mass in the catalytic layer. The Nafion[®]/carbon mass ratio of the ink used to prepare the MEAs was fixed at 0.5. After a standardized start-up procedure, polarization curves, *i.e.* the U_{cell} vs. current curves, were measured by setting the cell voltage at each desired value for 15 min, which ensured the stabilization of the current. The current was normalized either to the electrode surface (j_s) or to the Pt loading of the cathode (j_m).

3. RESULTS AND DISCUSSION

3.1. Characteristics of the Pt/carbon xerogel catalysts

Fig. 2 shows an example of TEM micrograph and the corresponding Pt particle size distribution, obtained by image analysis, of a Pt/carbon xerogel catalyst. This catalyst was obtained by three consecutive impregnation-drying-reduction cycles performed on a support with a macropore size ranging from 50 to 85 nm, a specific surface area of 640 m² g⁻¹ and a total pore volume of about 2.1 cm³ g⁻¹ (including 0.26 cm³ g⁻¹ of micropores, *i.e.* pores smaller than 2 nm). The results show that repeating the impregnation with H₂PtCl₆ as Pt precursor yields to an increase of the catalyst metal content while keeping homogeneously dispersed Pt nanoparticles *ca.* 2 nm in size. The number of impregnation cycles does not modify the metal dispersion. After three impregnation cycles, the Pt weight percentage of the catalyst was equal to 22.3 wt.%. Similar results were found using carbon xerogels with other pore textures (smaller or larger pores, various pore volumes).

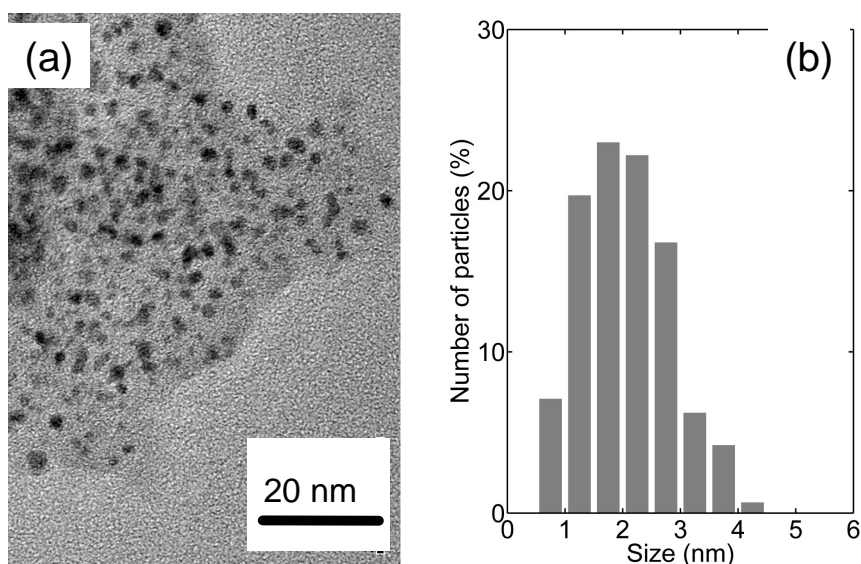


Figure 2. (a) TEM micrograph of a Pt/carbon xerogel catalyst and (b) particle size distribution obtained by image analysis. Sample prepared by SEA method, triple impregnation (22.3 wt.% Pt).

Table 1. Physico-chemical and electrochemical characterization of Pt/carbon xerogel catalysts reduced under various conditions. The catalysts were prepared *via* the SEA method (double impregnation, 15.0 wt.% Pt). $S_{\text{CO-strip}}$ (1) and $S_{\text{CO-strip}}$ (7) represent the real surface area estimated by integrating the charge required to oxidize a CO monolayer after one/seven CO_{ads} stripping, respectively.

Reduction conditions	TEM	XPS	CO stripping		ORR	
	d_{TEM}	Cl/Pt	$S_{\text{CO-strip}}$ (1)	$S_{\text{CO-strip}}$ (7)	b	SA_{90}
	(nm)	(-)	($\text{m}^2 \text{g}_{\text{Pt}}^{-1}$)	($\text{m}^2 \text{g}_{\text{Pt}}^{-1}$)	(V dec^{-1})	($\mu\text{A cm}^2_{\text{Pt}}^{-1}$)
200°C – 1 h	1.8 ± 0.2	$0.33 \pm 10\%$	$37 \pm 10\%$	$69 \pm 10\%$	$-0.074 \pm 5\%$	$10 \pm 5\%$
350°C – 3 h	1.8	0.23	61	87	-0.070	11
450°C – 5 h	1.8	0.07	129	142	-0.066	12

The metal dispersion observed by TEM is excellent. However, it is noteworthy that the final reduction temperature of the catalysts must be increased up to 450°C (5 h) to remove chlorine species coming from the metal precursor. Indeed, XPS measurements on catalysts reduced under various temperature conditions show that the Pt surface remains poisoned by chlorine when the reduction temperature is too low [9]. The relationship between the Cl/Pt ratio and the Pt surface detected by CO stripping, $S_{\text{CO-strip}}$, is linear (Fig. 3a). This means that, due to Cl poisoning, the electroactive Pt surface is lowered compared to that calculated from TEM; this induces a dramatic decrease of the cell performance when the catalyst is reduced at low temperature (Fig.3b). Note that increasing the reduction temperature up to 450°C does not induce any change in the Pt particle size: additional experiments have shown that the Pt nanoparticles begin to sinter at 650°C. Note also that consecutive CO stripping measurements can highlight the poisoning of the catalysts by Cl. Indeed, the detected Pt surface increases with the number of CO stripping procedures [9]; chlorine species are progressively removed by repetitive adsorption/desorption processes. In addition, the CO electrooxidation peak is shifted to more positive potentials when the reduction temperature decreases [9]. This may be ascribed to the competition between water and chloride species for the Pt adsorption sites. Indeed, previous studies [15, 16] have suggested that only a fixed number of active sites are able to form OH species and to initiate the CO electrooxidation kinetics on the Pt surface. Competitive adsorption by Cl species decreases artificially the number of active sites and shifts both the onset and the main CO electrooxidation peak towards positive potentials.

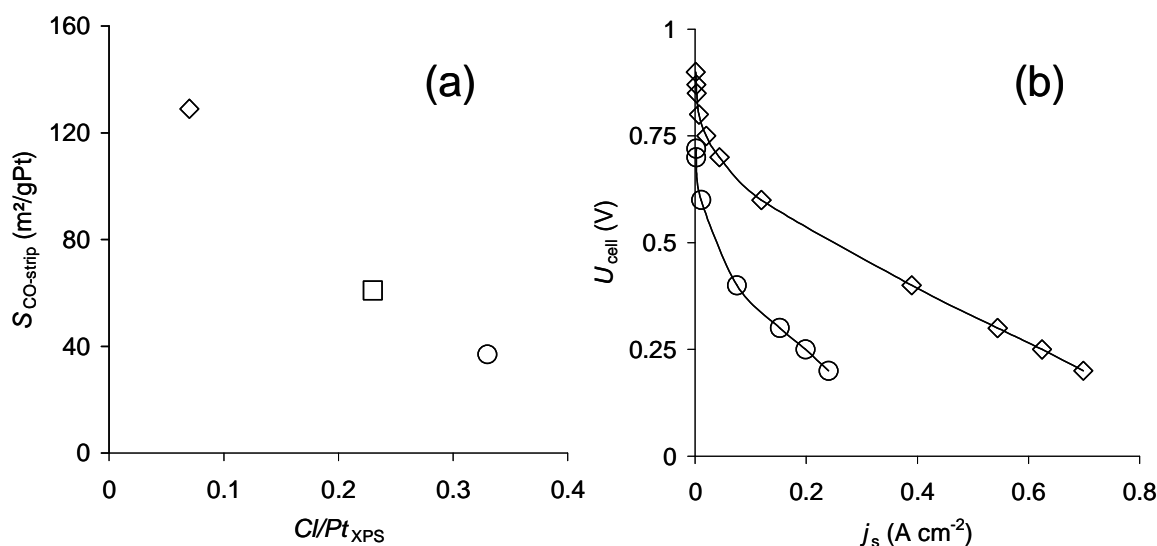


Figure 3. (a) Relationship between the Cl/Pt ratio detected by XPS and the Pt active surface measured by CO stripping (first measurement) for Pt/carbon xerogel catalysts obtained *via* the SEA method (double impregnation, 15 wt.% Pt) and reduced at 200°C for 1 h (○), 350°C for 3 h (□) and 450°C for 5 h (◇). (b) Effect of the Cl poisoning on the performance of an H_2/air cell: polarization curves at 70°C for MEAs with cathode processed with the same catalysts.

Oxygen Reduction Reaction (ORR) experiments performed in rotating disk electrode show that the presence of chlorine has little effect on the intrinsic reactivity of the Pt sites. Neither b nor SA_{90} changes significantly with the reduction treatment (Table 1), indicating that the reaction mechanism and kinetics remain the same. The only difference between the three samples is the accessible Pt surface, which decreases due to Cl poisoning when the reduction temperature is too low. In that extent, it is interesting to note that the sites that are not accessible in CO stripping experiments are not accessible either in ORR experiments.

3.2. Architecture and performance of cathodes designed with Pt/carbon xerogel catalysts

A catalytic layer of a typical PEM fuel cell electrode is composed of Pt/carbon black catalyst particles, interparticle voids and ionomer, hot-pressed between a proton-exchange membrane and a diffusion layer (carbon felt) [4]. To be active, the Pt particles must be in contact with the carbon support and connected to the membrane *via* the ionomer (Nafion[®]). In addition, reactants and products must circulate easily through the catalytic layers. In practice, a large fraction of the Pt can be inactive due to (i) a lack of contact between Pt and Nafion[®], (ii) the presence of liquid water within the pores of the cathode and (iii) mass transport limitations. As carbon black particles are loosely bonded and packed together in aggregates, the pore structure of the catalytic layer not only depends on the nature of the carbon black, but also on the electrode processing. On the contrary, the meso/macropore texture of catalytic layers prepared from carbon gels is totally independent on the electrode processing and can be regulated by choosing correctly the composition of the pristine wet gel. In the electrode structure, the carbon black particle agglomerates are replaced by micromonoliths of carbon gel made of covalently bonded carbon nodules, which preserves the pores located in-between (Fig. 4).

Membrane-Electrode Assemblies (MEAs) were prepared with carbon xerogels of various pore textures as cathodic catalyst supports and tested in an air/H₂ monocell device at 70°C. The aim of these tests was to highlight the effect of the pore texture on the diffusion overpotential. Indeed, the total voltage losses of the cell with regard to the reversible H₂/O₂ cell voltage can be decomposed into several components [17]: (i) the cathode overpotential, η_{ORR} , due to the sluggishness of the O₂ reduction kinetics; (ii) the ohmic losses, η_{Ohm} , due to the resistance of the proton migration through the membrane and ionomer within the electrodes, the electronic contact resistances between the flow-fields plates and the diffusion media, and the contact between the carbon grains; (iii) the mass-transport losses, or ‘diffusion overpotential’, η_{diff} , induced by slow O₂ diffusion through the diffusion layer and the catalytic layer. In such systems, kinetic and mass transport losses of the anode can be neglected [17]. η_{ORR} was obtained from measurements at low current densities, *i.e.* from data obtained in the near-absence of mass transport limitations and ohmic resistance; η_{Ohm} was obtained by measurement of the ohmic resistance of the cell by impedance spectroscopy, performed *in situ*;

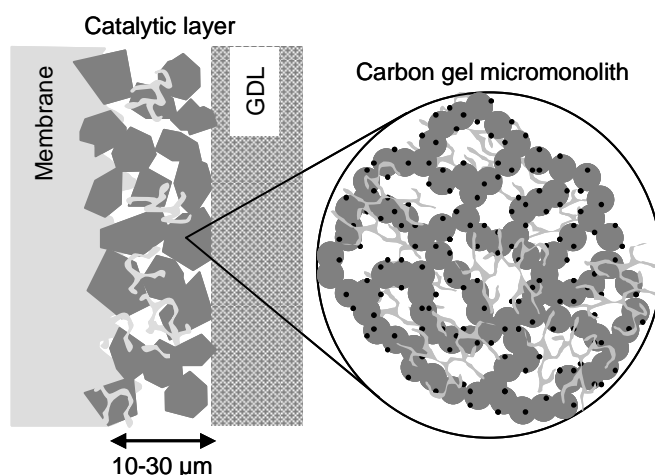


Figure 4. Structure of a PEM fuel cell electrode with carbon xerogel as catalyst support: the catalytic layer is composed of carbon gel micromonoliths made of a rigid 3D structure, insensitive to compression and with a defined pore texture. The Nafion[®] network and Pt particles are represented in light grey and black, respectively.

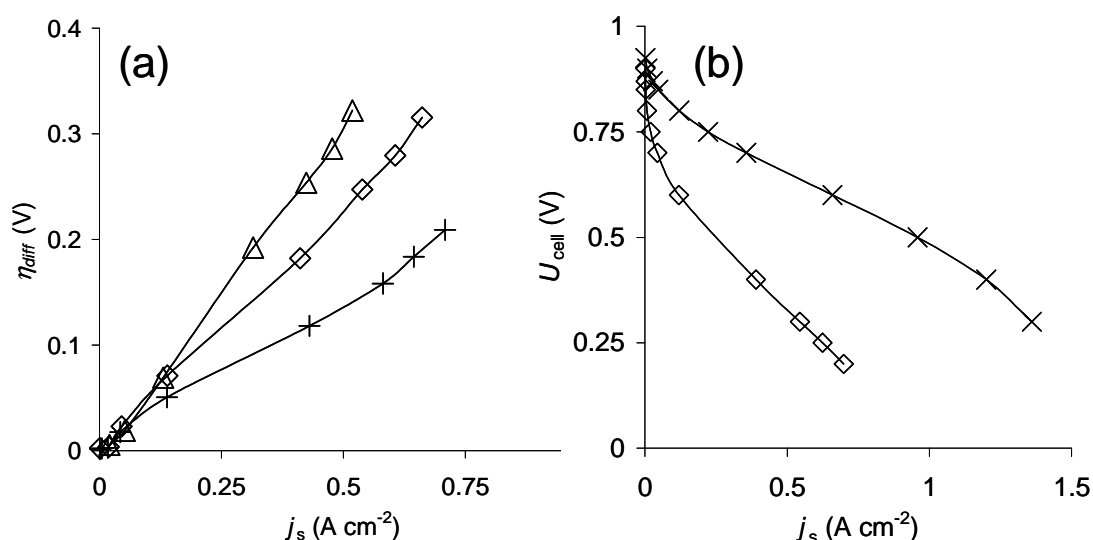


Figure 5. (a) Diffusion overpotential, η_{diff} , vs. experimental current density per surface unit of electrode. MEAs prepared with different carbon gel supports at the cathode: (Δ) mesoporous carbon xerogel (pore size \sim 20-25 nm), (\diamond) carbon xerogel with small macropores (pore size \sim 50-85 nm), (+) carbon xerogel with large macropores (pore size \sim 250-300 nm). (b) Polarization curves at 70°C for MEAs with cathode processed with (\diamond) carbon xerogel (pore size \sim 50-85 nm), SEA method (double impregnation, reduction under H₂ flow at 450°C), Pt loading = 0.15 mg_{Pt} cm⁻², (\times) Pt/carbon black (TKK, commercial electrode prepared by Paxitech), Pt loading = 0.60 mg_{Pt} cm⁻².

η_{diff} was calculated by difference. Fig. 5a shows the evolution of the diffusion overpotential with the pore texture of the carbon support: as the pore size increases, η_{diff} decreases, which clearly shows the impact of the cathode architecture on the electrode performance.

The global performance of the MEAs prepared with Pt/carbon xerogel catalysts at the cathode side was compared to that of a MEA using a commercial catalytic layer at both electrodes. In all cases, the commercial catalyst used was made from Pt-doped carbon black (40 wt.%, TKK), and the catalytic layers were prepared by Paxitech *via* deposition onto a carbon felt (Pt loading: 0.60 mg_{Pt} cm⁻²). In the case of Pt/carbon xerogel catalyst, the selected support was the carbon with 50-85 nm pores, and the Pt loading of the cathode was 0.15 mg_{Pt} cm⁻². Fig. 5b shows the polarization curves for the two MEAs: the global performance of the MEA prepared with the Pt/carbon xerogel catalyst remains lower than that of the commercial electrode. However, since the cathodic catalytic layer prepared with the Pt/carbon xerogel catalyst contains much less Pt (0.15 mg_{Pt} cm⁻²), the current should be normalized to the mass of Pt on the cathode (j_m) to compare the mass activity of the catalysts, and thus the utilization ratio of the precious metal. The results (not shown) indicate that both electrodes display quite similar performances in the so-called 'kinetic' region ($j_m < 1$ kA g_{Pt}⁻¹), where the mass-transport limitations are negligible. As a consequence, the intrinsic mass activities of the Pt nanoparticles in these two electrodes are close, which points to no dramatic difference in the morphology of the Pt particles. On the contrary, in the mass-transport controlled region ($j_m > 1$ kA g_{Pt}⁻¹), the Pt utilization is clearly higher in the case of the SEA catalyst supported on carbon xerogel. Such performance enhancement can be attributed to (i) the decrease of mass transport limitations and (ii) to the improvement of Pt-Nafion[®] contact, both inherent to the carbon texture.

4. CONCLUSION

Carbon xerogels are nanostructured carbon materials prepared by evaporative drying and pyrolysis of resorcinol-formaldehyde aqueous gels. These very clean carbon materials can advantageously replace carbon blacks as catalyst support for PEM fuel cell cathode, because their pore texture can be regulated so as to minimize mass transfer limitations within the catalytic layer. The pore size and void fraction of the

catalyst support are determining in the mass transport phenomena, and both parameters can be tuned *via* the pristine gel composition and drying procedure.

Pt/carbon xerogel catalysts with high metal content can be synthesized *via* the ‘Strong Electrostatic Adsorption’ method. By repeating the impregnation-drying-reduction step with H₂PtCl₆ as Pt precursor, it is possible to increase the catalyst metal content up to acceptable values (> 20 wt.%) while keeping a high metal dispersion (nanoparticles of homogeneous size, *ca.* 2 nm). However, the use of H₂PtCl₆, which is a very classical impregnation precursor, yields poisoning of the Pt catalysts by chlorine species which are quite difficult to remove completely. Even after reduction under H₂ at 450°C for 5 h, Cl is still detected *via* XPS measurements and electrochemical methods. The presence of chlorine does not modify the intrinsic activity of the metal: the reaction mechanism and kinetics remain the same. However, the electroactive surface of the Pt particles decreases due to its blocking by chlorine species; this can dramatically reduce the Pt utilization ratio in the PEMFC catalytic layer. The reduction step is thus determining in the catalyst preparation.

ACKNOWLEDGEMENTS

The authors wish to thank Dr Sophie Hermans, from the Institute of Condensed Matter of the Catholic University of Louvain (Belgium) for the XPS measurements.

REFERENCES

1. Gasteiger, H.A., Kocha, S.S., Sompalli, B., Wagner, F.T., 2005, *Appl. Catal. B*, vol. 56, n°1-2, pp. 9-35.
2. M. Chatenet, L. Dubau, N. Job, F. Maillard, *Catal. Today*, 156 (2010) 76–86.
3. Boehm, H.P., 1958, *Z. Anorg. Allg. Chem.*, vol. 297, pp. 315.
4. Hess, M.H., Herd, C.R., Carbon Black, *J.B. Donnet, R.C. Bansal, M.J. Wang*, Marcel Dekker, New York, 1993, pp. 89-174.
5. Job, N., Pirard, R., Marien, J., Pirard, J.-P., 2004, *Carbon*, vol. 42, n°3, pp.619-628.
6. Job, N., Théry, A., Pirard, R., Marien, J., Kocon, L., Rouzaud, J.-N., Béguin, F., Pirard, J.-P., 2005, *Carbon*, vol. 43, n°12, pp. 2481-2494.
7. Job, N., Heinrichs, B., Lambert, S., Pirard, J.-P., Colomer, J.-F., Vertruyen, B., Marien, J., 2006, *AIChE J.*, vol. 52, n°8, pp. 2663-2676.
8. Job, N., Marie, J., Lambert, S., Berthon-Fabry, S., Achard, P., 2008, *Energ. Convers. Manage.*, vol. 49, n°9, pp. 2461-2470.
9. Job, N., Lambert, S., Chatenet, M., Gomme, C.J., Maillard, F., Berthon-Fabry, S., Regalbuto, J.R., Pirard, J.-P., 2010, *Catal. Today*, vol. 150, n°1-2, pp. 119–127.
10. Regalbuto, J.R., *Catalyst Preparation: Science and Engineering*, 2007, *J.R. Regalbuto*, CRC Press, Taylor & Francis Group, Boca Raton, p. 297.
11. Lambert, S., Job, N., D’Souza, L., Pereira, M.F.R., Pirard, J.-P., Figueiredo, J.L., Heinrichs, B., Pirard, J.-P., Regalbuto, J.R., 2009, *J. Catal.*, vol. 261, n°1, pp. 23-33.
12. Maillard, F., Eikerling, M., Cherstiouk, O.V., Schreier, S., Savinova, E., Stimming, U., 2004, *Faraday Discuss.*, vol. 125, pp. 357-377.
13. Maillard, F., Schreier, S., Hanzlik, M., Savinova, E.R., Weinkauff, S., Stimming, U., 2005, *Phys. Chem. Chem. Phys.*, vol. 7, n°2, pp. 385-393.
14. Bard, A.J., Faulkner, L.R., *Electrochemical methods: fundamentals and applications*, 1992, Wiley, New-York, p.283.
15. Maillard, F., Savinova, E.R., Stimming, U., 2007, *J. Electroanalytical Chem.*, vol. 599, n°2, pp. 221-232.
16. Andreaus, B., Maillard, F., Kocylo, J., Savinova, E.R., Eikerling, M., 2006, *J. Phys. Chem. B*, vol. 110, n°42, pp. 21028-21040.
17. Gasteiger, H.A., Gu, W., Makharia, R., Mathias, M.F., Sompalli, R., *Handbook of Fuel Cells – Fundamentals, Technology and Applications*, 2003, *Vielstich, W., Lamm, A., Gasteiger, H.A.*, Wiley, Chichester (UK), vol. 3, p. 593.